JBC RESEARCH ARTICLE

The balance between nuclear import and export of NLRC5 regulates MHC class I transactivation

Received for publication, May 29, 2023, and in revised form, February 8, 2024 Published, Papers in Press, March 20, 2024,
https://doi.org/10.1016/j.jbc.2024.107205

Baohui Zhu[1], **Ryota Ouda**[1], **Ning An**[1], **Tsutomu Tanaka**[1,2], **and Koichi S. Kobayashi**[1,2,3,*]

From the [1]*Department of Immunology, Hokkaido University Graduate School of Medicine, Sapporo, Japan;* [2]*Institute for Vaccine Research and Development (HU-IVReD), Hokkaido University, Sapporo, Japan;* [3]*Department of Microbial Pathogenesis and Immunology, Texas A&M Health Science Center, Bryan, Texas, USA*

Reviewed by members of the JBC Editorial Board. Edited by Clare E. Bryant

Major histocompatibility complex (MHC) class I molecules play an essential role in regulating the adaptive immune system by presenting antigens to CD8 T cells. CITA (MHC class I transactivator), also known as NLRC5 (NLR family, CARD domain-containing 5), regulates the expression of MHC class I and essential components involved in the MHC class I antigen presentation pathway. While the critical role of the nuclear distribution of NLRC5 in its transactivation activity has been known, the regulatory mechanism to determine the nuclear localization of NLRC5 remains poorly understood. In this study, a comprehensive analysis of all domains in NLRC5 revealed that the regulatory mechanisms for nuclear import and export of NLRC5 coexist and counterbalance each other. Moreover, GCN5 (general control non-repressed 5 protein), a member of HATs (histone acetyltransferases), was found to be a key player to retain NLRC5 in the nucleus, thereby contributing to the expression of MHC class I. Therefore, the balance between import and export of NLRC5 has emerged as an additional regulatory mechanism for MHC class I transactivation, which would be a potential therapeutic target for the treatment of cancer and virus-infected diseases.

Major histocompatibility complex (MHC) molecules are critical to present antigenic peptides to T cells to activate adaptive immunity (1, 2). MHC class I mainly presents intracellular antigens to CD8 T cells whereas MHC class II mostly presents antigens from extracellular sources to CD4 T cells (3, 4). Since the expression level of MHC molecules is important to elicit the optimum immune responses against pathogens or cancer (5, 6), their expression is tightly regulated.

Recent research has identified NLRC5 (NLR family, CARD domain-containing 5) as a CITA (MHC class I transactivator) (7). NLRC5 is an IFNγ-inducible gene that belongs to the Nod-like receptor (NLR) or nucleotide-binding domain (NBD), leucine-rich repeats (LRRs) family of proteins (8). Similar to other NLR proteins, NLRC5 has a tripartite domain structure (9, 10); caspase recruitment domain (CARD) at its N terminal contains a bipartite nuclear localization signal (NLS) which is required for the nuclear translocation (11). The centrally located NACHT contains a nucleotide-binding motif, Walker A that is involved in the transactivation as well as nuclear importation of NLRC5 (12). The LRRs at the C terminus are generally known to mediate protein–protein interactions or ligand binding (13, 14). Among the NLR family proteins, NLRC5 is the largest member, possessing unusually long LRRs. However, the function of these LRRs remains poorly understood (15).

Though most NLR proteins are known to be located in the cytoplasm, two members of the family, CIITA (MHC class II transactivator) and NLRC5, have been reported to be translocated into the nucleus. CIITA is a master regulator of MHC class II gene expression (16–19), and the localization of CIITA between the cytoplasm and nucleus is balanced by the presence of NLS and nuclear export signal sequences (NES) (20). NLRC5 shuttles between the cytosol and nucleus, and its entry into the nucleus is essential for the transactivation of MHC class I genes (11). However, the regulatory mechanism of NLRC5 shuttling remains unclear. A thorough understanding of the transactivating function of NLRC5 on MHC class I requires a detailed examination of its mechanism for nuclear-cytoplasmic shuttling.

Functional nuclear proteins are required to be transported into the nucleus through the nuclear pore complex (NPC) by a process mediated by NLS signals. The importin α family, which includes KPNA1 (karyopherin alpha 1), KPNA2 (karyopherin alpha 2), KPNA3 (karyopherin alpha 3), KPNA4 (karyopherin alpha 4), KPNA5 (karyopherin alpha 5), KPNA6 (karyopherin alpha 6), and KPNA7 (karyopherin alpha 7), is capable of recognizing the NLS (21) and imports the proteins with NLS into the nucleus through the NPC by association with or without importin β (22–24). However, the specific domain or motif of NLRC5 that is crucial for importin recruitment remains unclear.

In addition to nuclear import, proper regulation of export is important for optimal protein localization in the nucleus. Chromosome region maintenance 1 (CRM1), also known as exportin 1, is a nuclear export receptor that recognizes and binds to NES present in cargo proteins to facilitate their export from the nucleus (25, 26). It has been reported that treatment with leptomycin B (LMB) (27), a well-known inhibitor of

* For correspondence: Koichi S. Kobayashi, kobayashi@tamu.edu, kskobayashi@med.hokudai.ac.jp.

CRM1-mediated nuclear export, results in a significant increase in the nuclear localization of NLRC5 (12), suggesting that NLRC5 export is a CRM1-dependent process.

In this study, we investigated the regulatory mechanisms underlying the import and export of NLRC5 utilizing molecular biology techniques. Our study revealed that each domain (CARD, NACHT, and LRR) of NLRC5 contributes to the regulation of nuclear import and export through distinct mechanisms and identified a novel histone acetyltransferases (HATs) that regulates the nuclear retention of NLRC5, resulting in increased MHC class I transactivation.

Results

IFNγ stimulation induces NLRC5 nuclear accumulation

IFNγ stimulation is a most potent inducer of the expression of NLRC5 and MHC class I genes (11, 28–31). Consistent with the previous studies by our and other groups, treatment with IFNγ resulted in a significant increase in the expression of MHC class I and related genes, *HLA-A*, *HLA-B*, and (Transporter associated with antigen processing 1 (*TAP1*), in *NLRC5*+/+ MCF7 cells while this induction was impaired in *NLRC5*−/− MCF7 cells, suggesting that the upregulation of MHC class I genes by IFNγ treatment was largely dependent on NLRC5 (Fig. S1*A*). Although this NLRC5 dependency is most likely due to the transcriptional upregulation of NLRC5 by IFNγ stimulation (11), we also observed that NLRC5 transfection and IFNγ stimulation cooperate to induce the expression of MHC class I genes (Fig. S1*B*), suggesting a possible mechanism to potentiate the activity of NLRC5 in the presence of IFNγ. Considering the critical role of nuclear import of NLRC5 in the activity as a CITA, we sought to investigate whether the IFNγ-induced MHC class I genes could be partially attributed to changes in the nuclear localization of NLRC5. The cellular localization of GFP-tagged NLRC5 upon IFNγ treatment was analyzed by immunofluorescence microscopy using the cells treated with a CRM1 inhibitor, LMB, which has been reported to inhibit the nuclear export of NLRC5 (11). Treatment with IFNγ induced the nuclear accumulation of NLRC5 and this accumulation was further enhanced by co-treatment with LMB (Fig. 1*A*). IFNγ-induced accumulation of NLRC5 in the nucleus was also confirmed by Western blotting (Fig. 1*B*). These results suggest that the increase in the activity of NLRC5 as a CITA upon IFNγ treatment was not only caused by transcriptional upregulation but also by an elevated accumulation of NLRC5 into the nucleus.

NLRC5 nuclear importation and retention contribute to enhanced MHC class I induction

To elucidate the significance of the localization of NLRC5 in the nucleus, we asked if blocking the nuclear importation or exportation of NLRC5 may impact the MHC class I gene transactivation. First, we examined the significance of nuclear localization of NLRC5 by using three NLRC5 expression vectors lacking NLS function; 1) CARD deleted mutant which lacks entire NLS, 2) mutant NLS-I in which the right arm of the bipartite NLS is mutated to alanine (RRK133/134/135A), and 3) mutant NLS-II in which the left arm of the bipartite NLS is mutated to alanine (KR121/122A) (Fig. 2*A*). Previous research indicated that mutation of a single arm of the NLRC5 bipartite NLS results in impaired function while retaining residual activity (12).

An increase in *HLA-A*, *HLA-B*, and *TAP1* mRNA expression was observed in WT NLRC5 overexpressing cells, but not in all of these mutant NLRC5-overexpressing cells (Fig. 2*B*), suggesting that NLRC5 translocation into the nucleus was required to elevate the transactivation of MHC class I genes. Second, the effect of elevated retention of NLRC5 in the nucleus on the transactivation of MHC class I genes was investigated by the blockage of NLRC5 exportation from the nucleus. Treatment of GFP-NLRC5–expressing cells with LMB resulted in the increased nuclear retention of NLRC5 in a time-dependent manner (Fig. S2*A*). Treatment with LMB induced the increase in *HLA-B*, beta-2-microglobulin (*B2M*), and *TAP1* promoter activity (Figs. 2*C* and S2*B*), and the transcription of HLA-B in a dose-dependent manner (Fig. 2*D*), and augmented surface expression of HLA-A, B, C (Figs. 2*F* and S2*C*) in HeLa and HEK293T cells, indicating that nuclear retention of NLRC5 may contribute to MHC class I transactivation. Co-treatment with LMB and IFNγ resulted in further enhanced *HLA-B* and *B2M* promoter activity in HEK293T cells (Fig. 2*C*) and increased HLA-B transcription in HeLa cells (Fig. 2*D*) and *NLRC5*+/+ MCF7 cells (Fig. 2*E*), while HLA-B expression was not augmented by the co-treatment in comparison to IFNγ treatment alone in *NLRC5*−/− MCF7 cells (Fig. 2*E*). Taken together, although IFNγ primarily induces MHC class I through transcriptional activation, these data suggest that nuclear retention and accumulation of NLRC5 may serve as an additional factor to increase the expression of genes in the MHC class I pathway.

The NLS in the CARD of NLRC5 is required for KPNA6 recruitment

The NLS in the CARD domain was required to import NLRC5 into the nucleus as shown above. Since the cargo proteins carrying NLSs are frequently transported into the nucleus through the NPC by an importin-dependent mechanism, we hypothesized that NLRC5 nuclear transport was also processed by importins. Immunofluorescence analysis showed that treatment with ivermectin, an inhibitor of the importin alpha/beta, resulted in a loss of nuclear localization of GFP-tagged NLRC5 in a dose-dependent manner, indicating that NLRC5 was translocated into the nucleus by an importin-dependent mechanism (Fig. S3).

Previous study reported that siRNA deletion of KPNA6, one of importin α members, resulted in impaired NLRC5 nuclear importation compared to control siRNA-treated cells (32). To study the significance of the NLS within the CARD domain of NLRC5 for the recruitment of KPNA6, HeLa cells were first co-transfected with expression vectors of HA-tagged KPNA6 and FLAG-tagged CARD, NACHT, or LRRs. Consistent with our hypothesis, a strong binding between KPNA6 and the

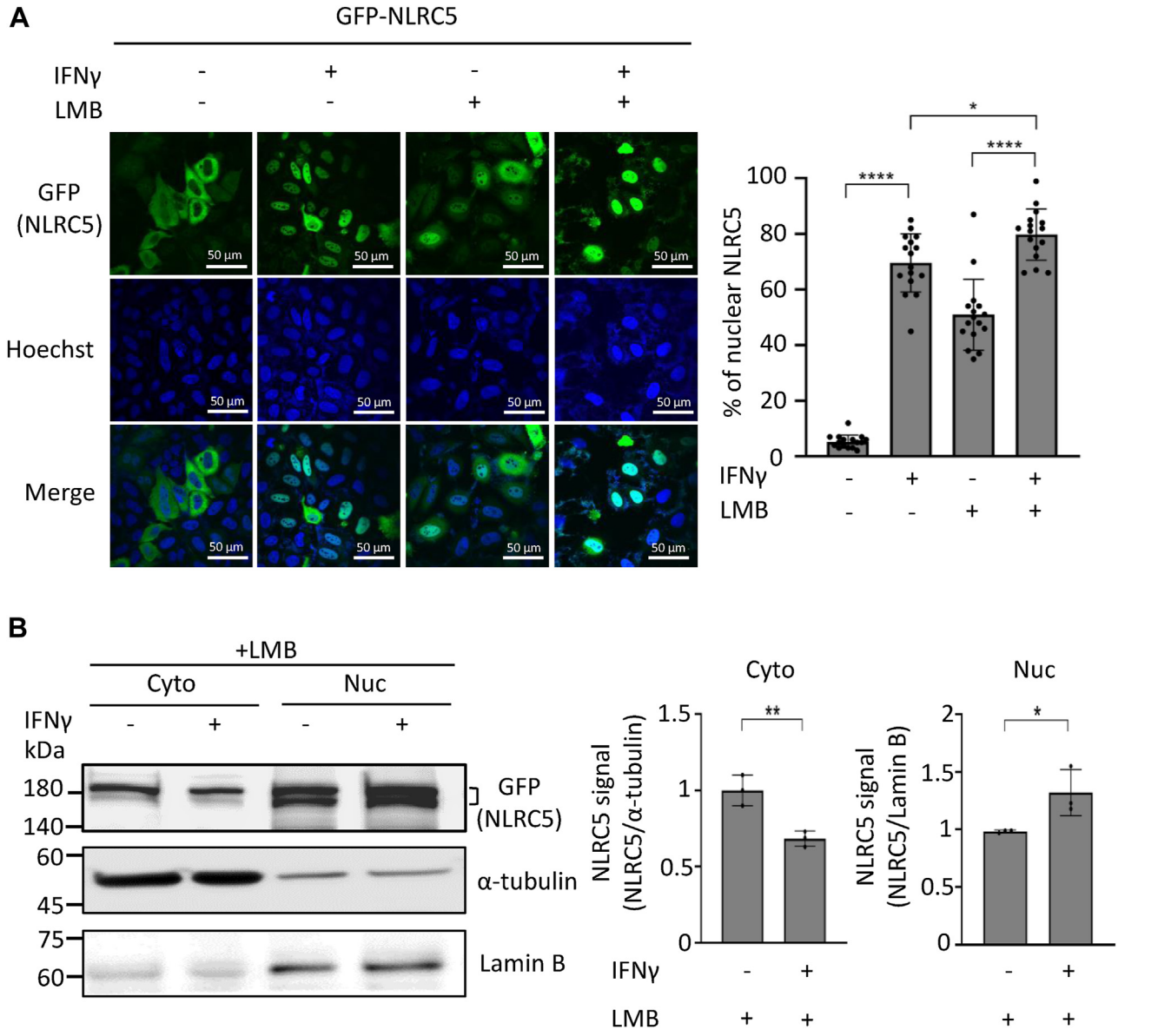

Figure 1. IFNγ induces nuclear accumulation of NLRC5. HeLa cells were transfected with a plasmid encoding GFP-tagged NLRC5 and cultured for 24 h. The transfected cells were stimulated with or without 200 U/ml IFNγ alone for 32 h, or LMB alone for 8 h, or treated with 200 U/ml IFNγ for 32 h in combination with LMB for the last 8 h. *A*, *left* panel representative images of the cellular localization of NLRC5. Cell nuclei were stained with Hoechst 33342. (*Right panel*) The bar graph indicates a quantitative comparison of the nuclear NLRC5 signal intensity, which was calculated as a percentage of the total cell signal intensity using ImageJ. The analysis was performed with 20 cells for each group. *B*, *left* panel the nuclear (Nuc) and cytoplasmic (Cyto) fractions were analyzed by Western blotting using anti-GFP, anti-α-tubulin, and anti-Lamin B antibodies. (*Right* panel) The bar graph shows a quantitative comparison of the cytoplasmic or nuclear GFP-NLRC5 signal intensity normalized by the intensity of α-tubulin (for cytoplasmic NLRC5) or Lamin B (for nuclear NLRC5) using ImageJ. Each experiment was performed three times independently, and the values shown are mean ± SD. *p*-values were calculated using Student's *t* test. $^{*}p < 0.05$, $^{**}p < 0.01$, $^{****}p < 0.0001$. NLRC5, NLR family, CARD domain-containing 5.

CARD was observed by immunoprecipitation analysis but not between KPNA6 and NACHT or LRRs (Fig. 3*A*), suggesting that CARD is a crucial domain in the association between KPNA6 and NLRC5. To further investigate the role of the NLS of NLRC5 in its association with KPNA6, HeLa cells were transfected by expression vectors for HA-tagged KPNA6 together with FLAG-tagged WT NLRC5, NLSI-mutated NLRC5 (NLSI-m), NLSII-mutated NLRC5 (NLSII-m), NLSI,II-mutated NLRC5 (NLSI,II-m), CARD deletion (△CARD), or CARD. While WT NLRC5 and CARD bound strongly to KPNA6, NLSI-m showed a reduced association with KPNA6. Additionally, NLSII-m, NLSI,II-m, and △CARD displayed even further reductions in the association (Fig. 3*B*). Collectively, these results demonstrate that both left and right arms of basic amino acid clusters of the bipartite NLS in the CARD contribute to the recruitment of KPNA6.

The Walker A motif of NLRC5 is important for the efficient recruitment of KPNA6

The NACHT domain of NLRC5 contains the Walker A motif which is essential for ATP binding (Fig. 4*A*). Previous

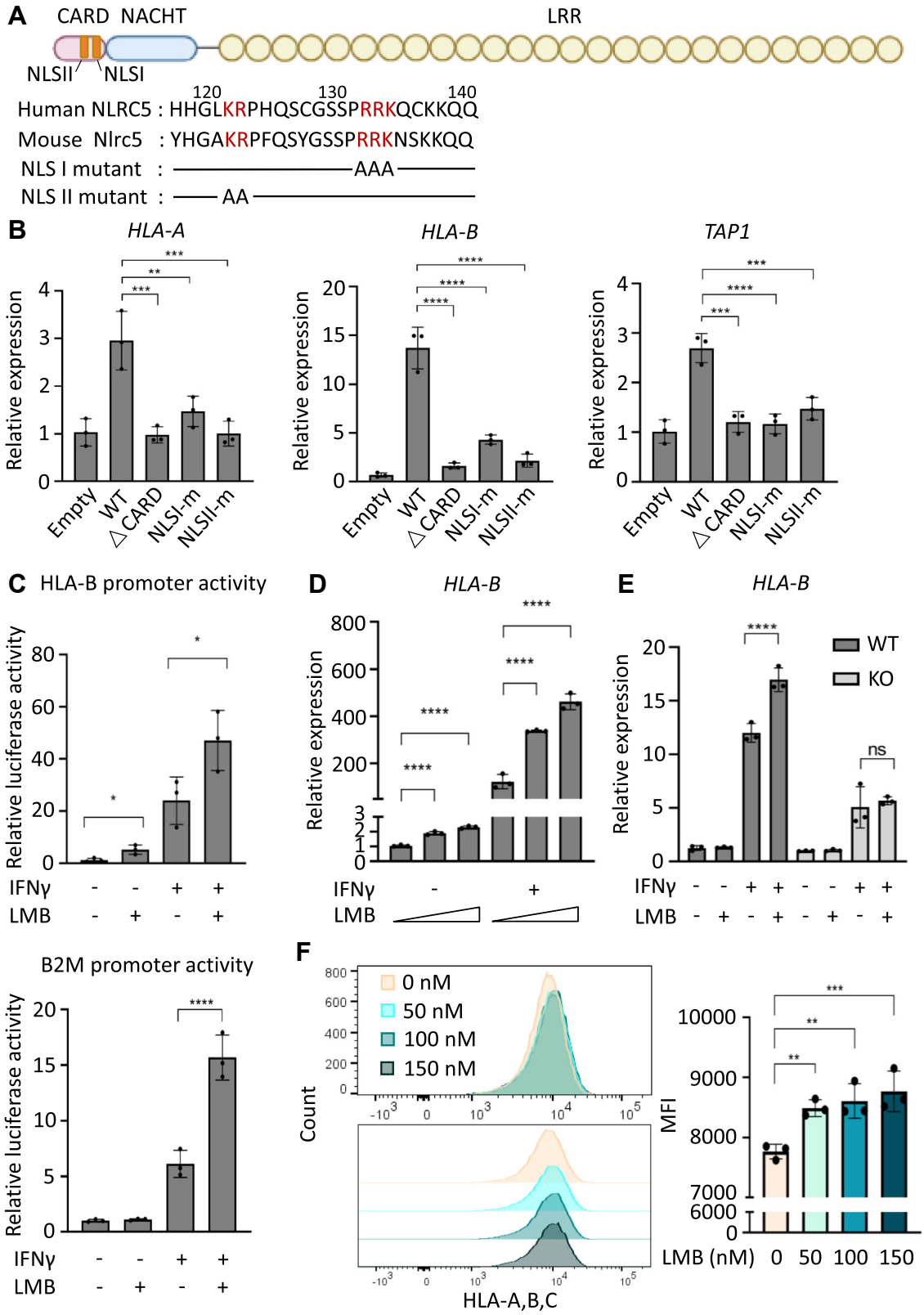

Figure 2. NLRC5 nuclear importation and retention contribute to MHC class I activation. *A*, schematic structure of NLRC5, indicating the CARD, NACHT, and LRRs domains. The bipartite NLS (NLS I and NLS II) is represented by *orange* boxes within the CARD, respectively. The amino acid sequences of both WT and mutant NLRC5 are displayed, with corresponding positions represented above. The bipartite NLS is highlighted in *red*. *B*, the mRNA level of MHC class I (*HLA-A* and *HLA-B*) and MHC class I–related genes in HEK293T cells transfected with plasmids encoding WT NLRC5, CARD-deleted NLRC5, or NLS-mutated NLRC5-encoding were quantified by RT-qPCR. *C*, HeLa cells were transfected with an NLRC5-dependent MHC class I promoter (HLA-B250)-luciferase reporter construct or a B2M promoter-luciferase construct. Twenty-four hours after transfection, the cells were stimulated with IFNγ (200 U/ml, 32 h) or LMB alone (100 nM, 8 h) or treated with IFNγ for 32 h in combination with LMB for the last 8 h. The luciferase activity was measured by dual-luciferase assay. Relative change to reporter-transfected, untreated HeLa cells was plotted. *D*, HeLa cells were stimulated with LMB (0, 50, or 100 nM, 8 h) alone or co-treated with

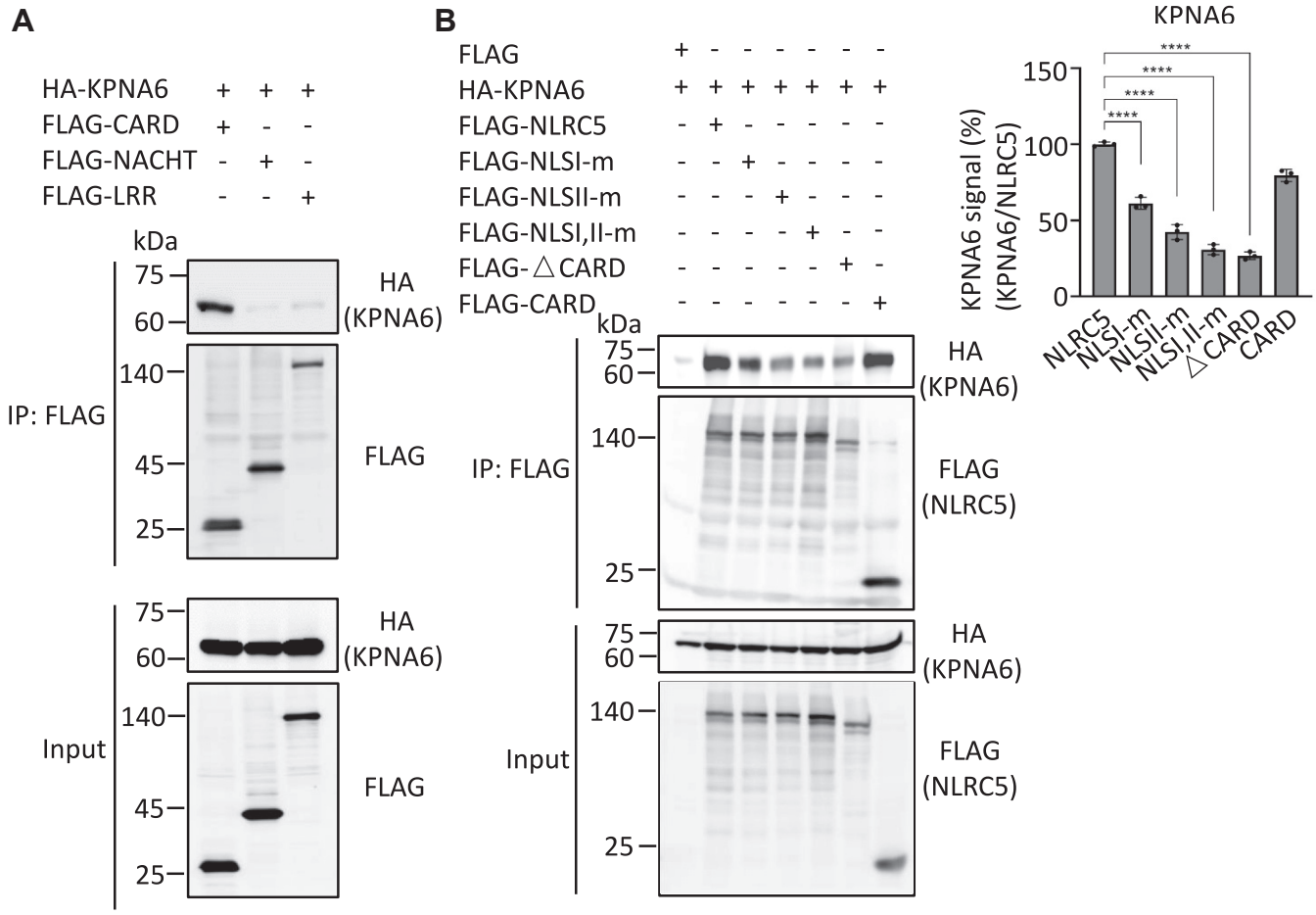

Figure 3. A bipartite NLS in the CARD of NLRC5 is required for association with KPNA6. *A*, HEK293T cells were co-transfected with a plasmid encoding HA-tagged KPNA6 and either a plasmid encoding FLAG-CARD, FLAG-NACHT, or FLAG-LRR. The transfected cells were harvested after 48 h, immunoprecipitated with anti-FLAG beads, and subjected to Western blotting using anti-HA and anti-FLAG antibodies. *B*, HEK293T cells were transfected with plasmids encoding FLAG-NLRC5, FLAG-NLSI-m (RRK133/134/135A), FLAG-NLSII-m (KR121/122A), FLAG-NLSI,II-m (KR121/122A, RRK132/133/134A), FLAG-△CARD, or FLAG-CARD along with HA-tagged KPNA6. (*Left* panel) The transfected cells were harvested after 48 h, immunoprecipitated with anti-FLAG beads, and subjected to Western blotting using anti-HA and anti-FLAG antibodies. (*Right panel*) Quantitative comparison of the KPNA6 signal intensity to that of NLRC5 is shown with a bar graph analyzed by ImageJ. Each experiment was performed three times independently. The values shown are mean ± SD. *p*-values were calculated using Student's *t* test. **** $p < 0.0001$. CARD, caspase recruitment domain; LRR, leucine-rich repeat; NLRC5, NLR family, CARD domain-containing 5; NLS, nuclear localization signal.

reports showed that the Walker A motif of NLRC5 is critical for both nuclear importation and transactivation of the MHC class I promoters (9, 10). Consistent with these studies, GFP-tagged mutant NLRC5 lacking either the NACHT domain or the Walker A motif failed to exhibit nuclear localization. (Fig. 4*B*). To explore if the Walker A motif plays a role in the association between NLRC5 and importin proteins, we conducted immunoprecipitation of KPNA6 with WT and Walker A mutant NLRC5. The results showed a strong binding between WT NLRC5 and KPNA6, whereas NLRC5 with the mutant Walker A motif (WAm) exhibited a weaker binding to KPNA6 (Fig. 4*C*). These data suggest that Walker A motif also contributes to the association between NLRC5 and KPNA6.

LRRs suppress the nuclear accumulation of NLRC5

NLRC5 contains the longest LRRs among all NLR protein members, and its functional role remains elusive. Given that the LRRs of CIITA are reported to be associated with its exportation from the nucleus to the cytoplasm (33), we hypothesized that the LRRs of NLRC5 might also play a similar role.

LMB (0, 50, or 100 nM, 8 h) following treatment with IFNγ (200 U/ml) alone for 24 h. *HLA-B* mRNA level was quantified using RT-qPCR. *E*, the *HLA-B* mRNA expression in *NLRC5*+/+MCF7 (WT) or *NLRC5*−/−MCF7 (KO) cells stimulated with or without IFNγ (200 U/ml, 32 h) alone, LMB (100 nM, 8 h) alone, or their combination was quantified using RT-qPCR. *F*, the surface expression of HLA-A/B/C on HEK293T cells co-treated with LMB (0, 50, 100, or 150 nM) and IFNγ (200 U/ml) for 8 h following treatment with IFNγ (200 U/ml) for 24 h was analyzed by flow cytometry. (*Left panel*) A histogram indicates the HLA-A/B/C expression on the cells treated with the indicated dose of LMB. (*Right panel*) The quantification of the mean fluorescence intensity (MFI) of HLA-A/B/C. Each experiment was performed three times independently, and representative result was shown. The values shown are mean ± SD. *p*-values were calculated using Student's *t* test. ns: not significant, * $p < 0.05$. ** $p < 0.01$, *** $p < 0.001$, **** $p < 0.0001$. B2M, beta-2-microglobulin; CARD, caspase recruitment domain; LRR, leucine-rich repeat; MHC, major histocompatibility complex; NLRC5, NLR family, CARD domain-containing 5; NLS, nuclear localization signal; RT-qPCR, quantitative reverse-transcription PCR.

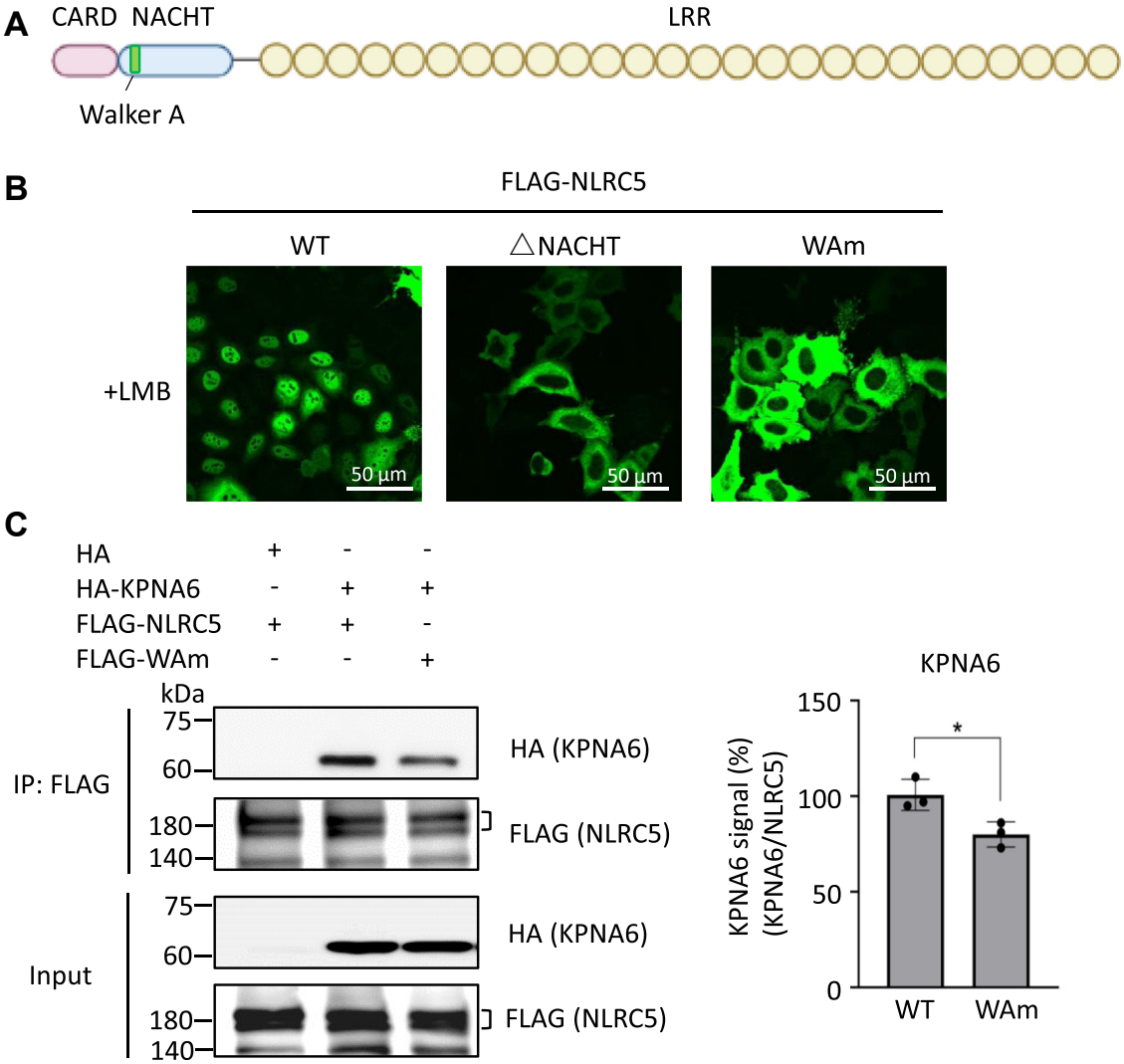

Figure 4. ATP binding is important for the efficient association of KPNA6 with NLRC5. *A*, schematic structure of NLRC5, indicating the CARD, NACHT, and LRRs domains of NLRC5. The Walker A motif in the NACHT domain is represented by the *green* box. *B*, representative image of the cellular localization of indicated NLRC5 protein. HeLa cells were transfected with the plasmids encoding FLAG-tagged WT NLRC5 (WT), NACHT-deleted NLRC5 (△NACHT), or walker A motif–mutated NLRC5 (WAm), cultured for 24 h, and then treated with 100 nM LMB for 8 h. *C*, HEK293T cells were transfected with plasmids encoding FLAG-tagged WT NLRC5 (FLAG-NLRC5) or walker A motif–mutated NLRC5 (FLAG-Wam) along with the HA-tagged KPNA6 vector. (*Left* panel) The cell lysates were prepared 48 h post-transfection, immunoprecipitated with anti-FLAG M2 beads, and subjected to Western blotting using anti-HA and anti-FLAG antibodies. (*Right* panel) Quantitative comparison of the KPNA6 signal intensity to that of NLRC5 is shown with a bar graph analyzed by ImageJ. Each experiment was performed three times independently. The values shown are mean ± SD. *p*-values were calculated using Student's *t* test. $*p < 0.05$. CARD, caspase recruitment domain; LRR, leucine-rich repeat; NLRC5, NLR family, CARD domain-containing 5.

To test this hypothesis, we first examined if NLRC5 associates with CRM1. We also examined which domains of NLRC5 associate with CRM1 by expressing individual domains with CRM1. We observed that the full length and LRRs of NLRC5 efficiently associated with CRM1, while the CARD and NACHT domains did not show significant binding (Fig. S4).

Second, we examined the role of LRRs in the cellular localization of NLRC5 by generating FLAG-tagged expression vectors for NLRC5 with different lengths of LRRs (Fig. S5*A*). Treatment with LMB (27), a well-characterized inhibitor of CRM1-mediated nuclear export, is reported to induce a significant increase in the nuclear localization of NLRC5 (12). Since treatment with LMB over 4 h results in the nuclear localization of even WT NLRC5 (Fig. S2*A*), the cellular localizations of those deletion mutant NLRC5 were examined by immunofluorescence microscopy after transfection followed by LMB treatment for 4 h. NLRC5 nuclear localization decreased as the length of LRRs increased (Fig. S5*B*), whereas lacking LRRs exhibited the most prominent localization in the nucleus and less association with CRM1 (Fig. S5*C*). These results suggest the length of the LRRs of NLRC5 plays an important role in manipulating NLRC5 cellular localization.

GCN5 promotes the nuclear accumulation of NLRC5 by blocking CRM1-dependent NLRC5 exportation

Since HATs were reported to promote NLRC5-induced MHC class I activation (34) and it has been shown that the nuclear accumulation of CIITA can be enhanced by one of the HATs,

PCAF (P300/CBP-associated factor) (35), we hypothesized that HATs may be involved in the regulation of nuclear accumulation of NLRC5. We selected three HAT members (PCAF, p300, and GCN5 (general control non-repressed 5 protein)) based on our previous observation for their ability to increase NLRC5-induced MHC class I gene activation (34). HeLa cells cotransfected with GCN5 and GFP-NLRC5 showed a significant increase in the nuclear accumulation of GFP-NLRC5, while cells transfected with PCAF or p300 did not show any increment of nuclear NLRC5 (Fig. 5*A*). This observation led us to consider the possible involvement of GCN5 for the inhibition of CRM1-mediated exportation of NLRC5. To test whether the association between NLRC5 and CRM1 was altered by the expression of GCN5, we performed immunoprecipitation analysis using cells transfected with the expression vectors for NLRC5 and CRM1 either alone or in combination with GCN5. While we found a strong association between NLRC5 and CRM1, a significant decrease in the association between CRM1 and NLRC5 was observed in the presence of GCN5 (Fig. 5*B*). This GCN5-mediated inhibition of the association between NLRC5 and CRM1 appeared dose-dependent as transfection with an increased dose of the GCN5 expression vector resulted in more prominent binding inhibition (Fig. S6*A*). To study the GCN5 function in promoting MHC class I gene induction, HeLa cells were transfected with expression vectors of HA tag or HA-tagged GCN5, stimulated with or without IFNγ, and then the expression of MHC class I and related genes was compared using quantitative reverse-transcription PCR (RT-qPCR). The mRNA expression of IFNγ-induced *HLA-A*, *HLA-B*, *TAP1*, and *B2M* were significantly upregulated in the presence of GCN5 (Fig. 5*C*). Moreover, the NLRC5-induced MHC class I promoter activity was also boosted by GCN5 (Fig. S6*B*). Together, those results suggest that GCN5 induces NLRC5 nuclear accumulation by interfering with the interaction between NLRC5 and CRM1, contributing to the upregulation of the expression of MHC class I genes.

Discussion

Effective regulation of the MHC class I pathway by NLRC5 is contingent upon its nuclear import (11, 12). This present study defines the mechanism of nuclear import and retention of NLRC5, highlighting the significance of three domains of NLRC5 in the nuclear translocation and revealing a novel regulator of the nuclear retention of NLRC5. As shown in Figures 3 and 4, the NLS in the CARD and the Walker A motif in the NACHT domain are important for the recruitment of an importin. Since ATP binding to the Walker A has been proposed to induce the conformational changes in NLR proteins (36, 37), these data may imply that ATP binding to the Walker A motif of NLRC5 induces its conformational changes, which may enhance the association between NLRC5 NLS and KPNA6. Moreover, we found that the LRRs exert a negative impact on the nuclear localization of NLRC5 in a length-dependent manner, suggesting the possible presence of multiple NES in the LRRs (Fig. S5*B*) (25). Indeed, the NES-binding nuclear export receptor CRM1 was associated with NLRC5 but exhibited reduced association with NLRC5 upon LRR deletions (Fig. S5*C*). This observation further suggests that the potential NESs located in the LRRs promoted the nuclear export of NLRC5 (Fig. 5*B*). Besides revealing the roles of the three domains in nuclear localization, we identified a novel regulator of nuclear retention, GCN5. A study reports that GCN5 interrupts the interaction of proteins to inhibit gene transcription (38). Consistently, GCN5 impeded the binding between NLRC5 and CRM1, resulting in the enhanced retention of NLRC5 in the nucleus (Fig. 5, *A* and *B*).

In summary, all domains of NLRC5 are involved in the mechanism of shuttling between the cytoplasm and the nucleus. This regulation is enabled by the presence of key molecular players, KPNA6, CRM1, and GCN5, in orchestrating the process of NLRC5 shuttling. Based on these observations, we propose the following model for the nuclear importation and exportation of NLRC5. In the cytoplasm, NLRC5 associates with KPNA6, one of the importin α members, facilitating its translocation into the nucleus through the nuclear pore complex (Fig. 6 left panel). The NLS in the CARD and active conformational changes in NLRC5 through ATP binding may enhance the association between NLRC5 and KPNA6. In the nucleus, CRM1 plays a pivotal role in steering the export of NLRC5 from the nucleus by associating the LRRs of NLRC5, creating cytoplasm-nuclear shuttling of NLRC5 (Fig. 6 left panel). In contrast, one of the HATs members, GCN5, emerges as an NLRC5 export inhibitor, disrupting the NLRC5–CRM1 interaction and placing a constraint on the nuclear export of NLRC5 (Fig. 6 right panel) in the nucleus generates CITA enhanceosome with other transcription factors at the proximal promoter of MHC class I and related genes, driving their transcription (Fig. 6 right panel).

This model, however, may need modifications during inflammation. As NLRC5 is relocalized into the nucleus by IFNγ, it is possible that the nuclear balance mechanisms of NLRC5 may be influenced by cytokines such as IFNγ produced during inflammation. While additional studies are required to clarify the link between altered mechanisms of localization balance of NLRC5 and IFNγ stimulation, our findings suggest that maintaining the balance of NLRC5 localization is important for appropriate MHC class I expression levels in both steady and inflammatory states.

NLRC5 and CIITA are both nuclear proteins and share the highest similarity among all NLR proteins upon phylogenetic analysis of the NACHT domain (11, 39). Regulatory mechanisms of nuclear localization of these two proteins also appear to be similar. First, among NLR members, they share phylogenetically the most similar NBD domains that are required for nuclear import (11, 40). Second, both CIITA and NLRC5 carry NLSs, which enable them to associate with importins and translocate into the nucleus (11, 20, 35) Third, both proteins contain LRRs at the C terminus, which is the common location for the NES, a critical site for the CRM1-dependent nuclear export (25, 41). Lastly, our findings indicate that HATs play a crucial role in the translocation of both NLRC5 and CIITA. Interestingly, the nuclear retention of NLRC5 and CIITA is regulated by different HATs *via* distinct mechanisms. PCAF and GCN5 are two closely related HATs (42) and both are known to acetylate histone proteins to promote transcriptional activation (42). In the case of CIITA, PCAF has been identified

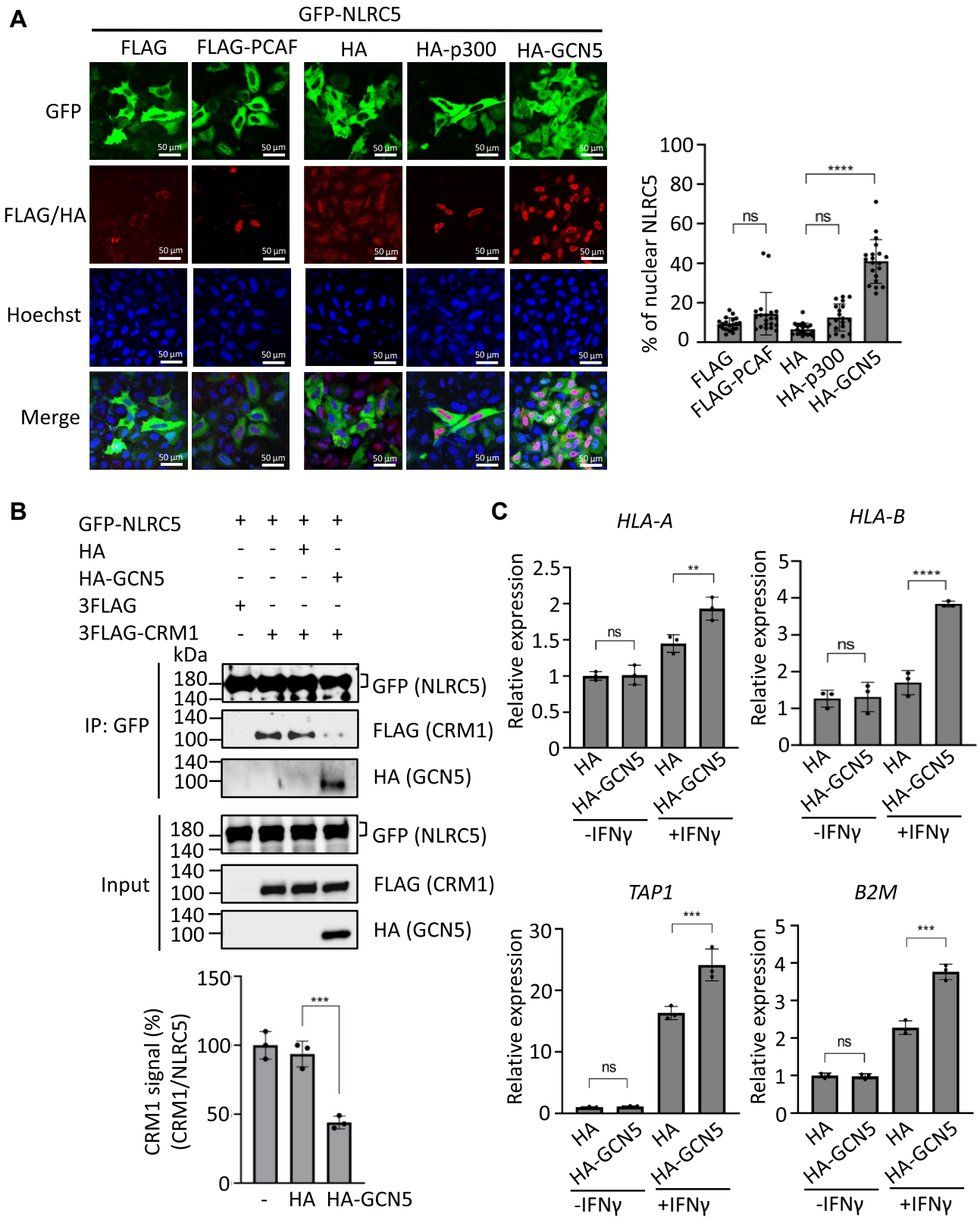

Figure 5. GCN5 induces nuclear retention of NLRC5 by interfering with NLRC5-CRM1 association. *A*, HeLa cells were transfected with the plasmid encoding GFP-tagged NLRC5 along with plasmids encoding the indicated FLAG- or HA-tagged proteins. (*Left* panel) 48 h after transfection, the cellar localization was analyzed by a confocal microscopy. Cell nuclei were stained with Hoechst 33342. (*Right* panel) The bar graph represents a quantitative comparison of the nuclear NLRC5 signal intensity, which was calculated as a percentage of the total cell signal intensity using ImageJ. The analysis was performed on 20 cells for each sample. *B*, HEK293T cells were transfected with the GFP-tagged NLRC5 encoding vector along with FLAG-tagged CRM1 and/or HA-tagged GCN5 encoding vectors and cultured for 48 h. Cell lysates were incubated with anti-GFP antibody overnight, then immunoprecipitated with protein A/G agarose beads. (*Upper* panel) Immunoprecipitated protein complexes were subjected to Western blotting using anti-GFP, anti-FLAG, and anti-HA antibodies. (*Lower* panel) The relative change of the intensity of CRM1 normalized by NLRC5 was shown with a bar graph. *C*, HEK293T cells were

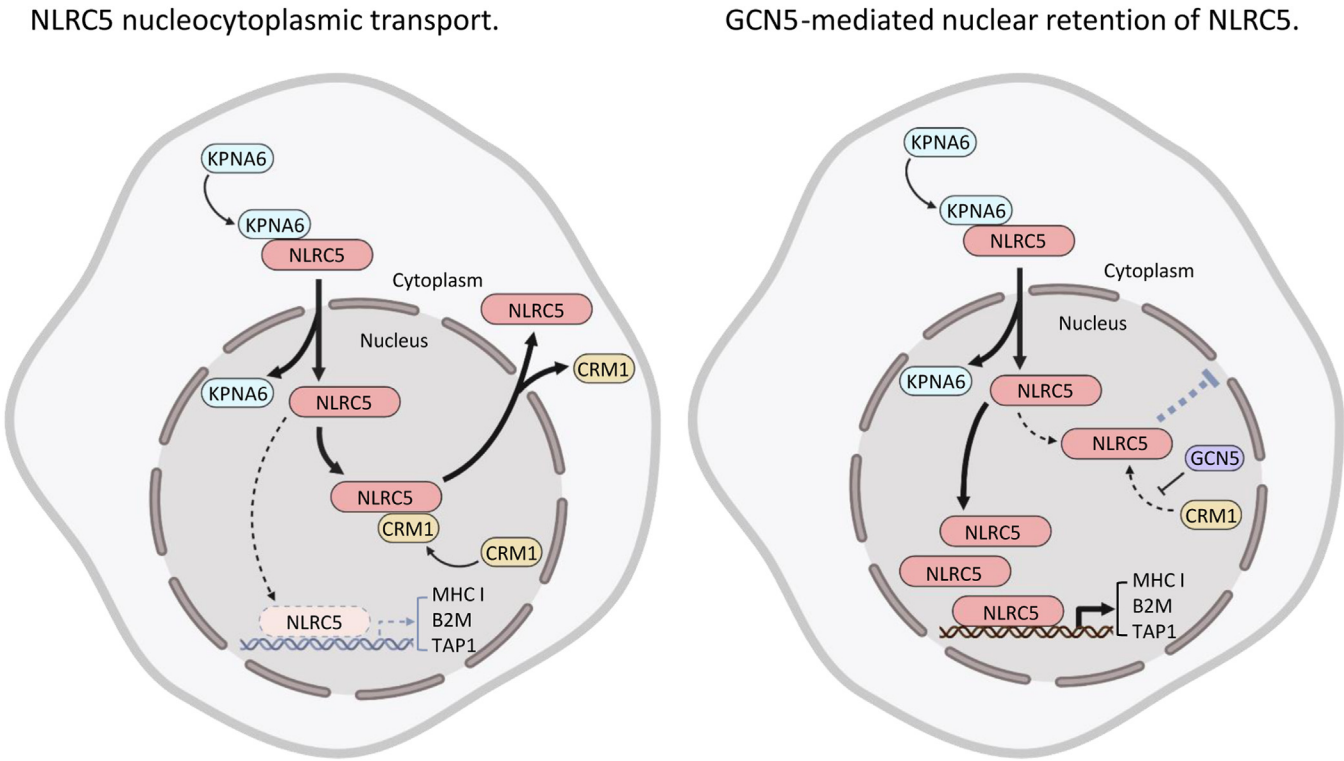

Figure 6. Schematic illustration of the mechanism of NLRC5 nuclear import and retention. NLRC5 is mainly located in the cytoplasm of the cell. NLRC5 is associated with KPNA6 in the cytoplasm and is imported into the nucleus through the nuclear pore. (*Left* panel) CRM1 binds NLRC5 resulting in the export of NLRC5 out of the nucleus through the nuclear pore. (*Right panel*) GCN5 inhibits the NLRC5-CRM1 binding, preventing NLRC5 export from the nucleus. The nuclear accumulation of NLRC5 induced by these mechanisms results in the transactivation of MHC class I genes. GCN5, general control non-repressed 5 protein; MHC, major histocompatibility complex; NLRC5, NLR family, CARD domain-containing 5.

as a major regulator, enhancing the nuclear accumulation of CIITA by inducing direct acetylation of CIITA (35). In the case of NLRC5, PCAF did not affect the nuclear localization (Fig. 5*A*). However, GCN5 emerged as a major HAT that regulates and induces the nuclear retention of NLRC5 by inhibiting its association with CRM1 (Fig. 5*B*).

In conclusion, our findings uncovered the molecular mechanisms underlying the nuclear import and retention of NLRC5. The observed enhancement of MHC class I gene expression due to the nuclear retention of NLRC5 (Fig. 2) implies that the intervention of the shuttling mechanism of NLRC5 could potentially be a therapeutic target for addressing virus infections and cancers. However, further research is necessary to fully understand the clinical implications and potential applicability of these findings.

Experimental procedures

Cell lines

HeLa, MCF7, and HEK293T cell lines were purchased from ATCC and cultured in Dulbecco's Modified Eagle Medium supplemented with 10% heat-inactivated fetal bovine serum (Nichirei, 175012) and penicillin-streptomycin (100 U/ml and 100 μg/ml, respectively, Nacalai Tesque, 09367-34) in a humidified incubator at 37 °C, 5% CO2. A human NLRC5-deficient stable cell line was generated by the CRISPR/Cas9 dual-gRNA knockout system. Two sgRNAs (gRNA-Fw: ATCCTTAGACACTCCGGAGGGGG, gRNA-Rv: CAGGCGACTTGGCACAGTGCGGG) targeting the NBD domain of NLRC5 were amplified together with the pH1-scaffold template and inserted into lentiCRISPR V2 vector to construct the lenti-gRNA plasmid. HEK293T cells were transfected with lenti-gRNA plasmid, pCMV-VSV-G, and psPAX2 plasmids to generate the lentivirus particles packaging sgRNAs. The supernatant was collected 48 h after transfection and filtered through a 0.45 μm filter (Sartorius Stedim, S7598-FXOSK). MCF7 cells on one well in a 12-well plate were incubated with 1 ml of the filtered supernatant and 5 μg polybrene (Nacalai Tesque, 12996-81) for 48 h, followed by selection with 3 μg/ml puromycin (Invivogen, 14861-71). The absence of NLRC5 expression in the generated cell line was confirmed by qPCR using NLRC5-specific primers (hNLRC5-Fw: CTGGCCAGTCTCACCGCACAA, hNLRC5-Rv: CCAGGGGACAGCCATCAAAATC).

Plasmids

GFP-tagged NLRC5 was generated as described previously (11). FLAG-tagged full-length NLRC5, CARD domain,

transfected with HA-empty or HA-GCN5 encoding plasmid, cultured for 24 h, and subsequently treated with 200 U/ml IFNγ for an additional 24 h. The mRNA levels of MHC class I (*HLA-A* and *-B*) and MHC class I–related genes (*TAP1* and *B2M*) were quantified by RT-qPCR. Each experiment was performed three times independently, and the values shown are mean ± SD. *p*-values were calculated using Student's *t* test. ns: not significant, ** $p < 0.01$, *** $p < 0.001$, **** $p < 0.0001$. B2M, beta-2-microglobulin; GCN5, general control non-repressed 5 protein; MHC, major histocompatibility complex; NLRC5, NLR family, CARD domain-containing 5; RT-qPCR, quantitative reverse-transcription PCR.

NACHT domain, LRR domain, and LRR deletion mutants (CARD+NACHT+LRR1-20 (C+N+LR1-20), C+N+LR1-15, C+N+LR1-10, C+N+LR1-5, NLRC5-ΔLRR) were generated by amplifying DNA fragments from GFP-tagged NLRC5 using PCR (primers: NLRC5-Fw: ATATCTAGAATGGACCCCG TTGGCCTCCAGCT, NLRC5-Rv: AAAGTCGACTCAAG-TACCCCAAGGGGCCTGGG, CARD-Fw: ATATCTAGAAT GGACCCCGTTGGCCTCCAGCT, CARD-Rv: AAAGTC-GACCTACGGGCCCTTGTTAACCCTGG, NACHT-Fw: GG GTCTAGAATGAGGGTGACCGTGCTTTTGGGGAA, NA CHT-Rv: ATAGTCGACCTACACCTGCACTACAGCAGCC TGCT, LRR-Fw: CACTCTAGAATGTTGAAGAAGTTGG CCACCCGCAA, LRR-Rv: ATAGTCGACCTACACCTGCAC TACAGCAGCCTGCT, LRR-deletion-Fw: ATATCTAGAAT GGACCCCGTTGGCCTCCAGCT, C+N+LR1-20-Rv: AAAG TCGACCTACAGCCCAGGCAGGATGGTAGCTA, C+N+ LR1-15-Rv: AAAGTCGACCTAGGACAGCAGGAGGCT CTGCAGCA, C+N+LR1-10-Rv: AAAGTCGACCTAGGGTC CCGGGCAGTCCTTCAGAGT, C+N+LR1-5-Rv: AAAGTC-GACCTACTGGGATGCAGCCTCTGCCATCA, NLRC5-ΔL RR-Rv: ATAGTCGACCTACACCTGCACTACAGCAGCC TGCT) and then cloning the fragments into p3xFLAG-CMV7.1 vector (Invitrogen) with XbaI and SalI. The HLA promoter pGL3-HLA-B (HLA-B250), TAP1 promoter and B2M promoters were kindly gifted from Dr van den Elsen (Leiden University, Netherlands) (43). FLAG-tagged C+N+LR1-4, C+N+LR1-3, C+N+LR1-2, C+N+LR1, NLRC5-ΔCARD, NLRC5-ΔNACHT, NLRC5-NLSI-m (RRK133/134/135A), NLRC5-NLSII-m (KR121/122A), NLRC5-NLSI,II-m (KR121/122A, RRK132/133/134A), and NLRC5-WAm were generated by Q5 Site-Directed Mutagenesis Kit (New England Biolabs, M0554S) using FLAG-tagged full length NLRC5 as a template (primers: NLRC5-muta-Fw: ATGTACCCA-TACGATGTTCC, C+N+LR1-4-Rv: TTCCTGGAGCAGG GCTAT, C+N+LR1-3-Rv: GTGAGGGAGAACCTCCAC, C+N+LR1-2-Rv: GAGAGGCAAAGCTTTCAC, C+N+LR1-Rv: TGTCGGCAAGCTCCTGGA, NLRC5-ΔCARD-Fw: AGG GTGACCGTGCTTTTG, NLRC5-ΔCARD-Rv: CATTCTA-GAGCGGCCGCC, NLRC5-ΔNACHT-Fw: TATGTTACC CTCCATTCCCG, NLRC5-ΔNACHT-Rv: CGGGCCCTTGT TAACCCT, NLSIm-Fw: GGCGCAGTGCAAGAAGCAG CAGC, NLSIm-Rv: GCCGCGGGTGAGGACCCACAGCT, NLSIIm-Fw: CCATGGCCTGGCGGCGCCACATCAGAG, NLSIIm-Rv: TGGAGCTGAGATTCAGGTTG, WAm-Fw: TGGCATGGGCgcgACCACGCTGG, WAm-Rv: GCCTT CCCCAAAAGCACG). HA-tagged KPNA6 was generated by amplifying a DNA fragment from pCMVTNT-T7-KPNA6 (Addgene plasmid number: 26682) and cloning it into a pcGN-HA vector (primers: KPNA6-Fw: AAAGAATTC GAGAC-CATGGCGAGCCCAGGGAAAGACAA, KPNA6-Rv: AAA TCTAGA TTATAGCTGGAAGCCCTCCATGGGGGCCT), which was kindly provided by Dr Shigetsugu Hatakeyama (Hokkaido University), using EcoRI and XbaI. PRC/RSV-FLAG-hPCAF and pcDNA3.1-HA-hGCN5 were kindly provided by Dr Peter van den Elsen. FLAG-CRM1 (#17647) and HA-p300 (#89094) were purchased from Addgene.

Flow cytometry

To analyze the surface expression level of HLA, 3×10^5 HEK293T cells were treated with 0, 50, 100, or 150 nM of LMB for 8 h. The single-cell suspensions were then stained with either PE-conjugated anti-human HLA-A, B, and C antibody (Biolegend, 311406) or PE-conjugated isotype control (Biolegend, 400213). After 30 min of incubation on ice, the cells were washed and resuspended in FACS buffer (2% fetal bovine serum/PBS) for analysis using a BD FACS Canto II flow cytometer. Data analysis was performed using FlowJo software (https://www.flowjo.com/solutions/flowjo).

Immunoprecipitation

For immunoprecipitation, 1.2×10^6 HEK293T cells were harvested 48 h after transfection with FuGENE HD (Promega, E2312) according to the manufacturer's protocol. The cells were incubated and sonicated in lysis buffer (150 mM NaCl, 20 mM Tris–HCl (pH 7.5), 0.1% NP40, 1 mM PMSF, protease inhibitor cocktail (Roche), and phosphatase inhibitor (Nacalai Tesque)), and cleared by centrifugation at 13,000 rpm for 10 min at 4 °C. For immunoprecipitation of FLAG-tagged protein complex, the cell extracts were incubated overnight with anti-FLAG M2 affinity gel (Sigma, F3165-1MG) at 4 °C. For immunoprecipitation of GFP-tagged protein complex, the cell extracts were gently mixed with anti-GFP antibody (Proteintech, 66002-1-Ig) overnight at 4 °C and then incubated with protein A/G agarose (Pierce) for 4 h at 4 °C. The immunoprecipitants were washed 3 times in ice-cold NP40 lysis buffer (0.1% NP40, 150 mM NaCl, 20 mM Tris–HCl (pH 7.5), 1 mM Na3VO4, 1 mM PMSF), resuspended in SDS sample buffer, boiled for 4 min at 95 °C. SDS-PAGE and blotting were performed as described below. Quantitative comparison of the band intensity was analyzed by ImageJ software (Image processing and analysis in Java, https://imagej.net/ij/). Western blotting images were converted into "Grayscale" picture mode by ImageJ software, and bands of interest were selected using the "rectangle" tool. The integrated density was measured for each region of interest and the graphs were generated using GraphPad Prism 9 software (https://www.graphpad.com/updates/prism-900-release-notes).

Subcellular protein fractionation

HeLa cells (6×10^5) were transfected with the GFP-NLRC5 expression vector, cultured for 24 h followed by IFNγ stimulation for another 24 h. Before harvesting, the cells were treated with 100 nM of LMB for 8 h. At 48 h post-transcription, the cells were washed twice with PBS and collected in cold lysis buffer (1 mM EDTA, 1 mM EGTA, 10 mM KCl, 1.5 mM MgCl2, 20 mM Hepes (pH 7.4), protease inhibitor cocktail (Roche, 11836170001), 1 mM DTT). After incubation for 15 min on ice, the cells were homogenized by passing through a 26-gauge needle ten times. Following incubation for 20 min on ice, the homogenate was centrifuged at 3000*g* for 10 min at 4 °C. The supernatant was transferred to a fresh tube as a cytoplasmic fraction, and the nuclear pellet was

washed with a fractionation buffer and then dispersed with a pipette and passed through a 25-gauge needle ten more times. The resuspended nuclear pellet was resuspended in a nuclear buffer (standard lysis buffer with 10% glycerol and 0.1% SDS added). The supernatant was collected after centrifuging at 10,000*g* and used as a nuclear fraction. The cytoplasmic and nuclear fractions were then analyzed by Western blotting with the protocol described below.

Western blotting

For Western blotting, samples were resolved by SDS-PAGE and transferred to polyvinylidene difluoride membranes (Merck, IPVH00010). After blocking with a blocking buffer (5% nonfat dried milk diluted in TBST), the membrane was incubated overnight with the following primary antibodies: anti-FLAG (Sigma, SL05105), anti-HA (B&D SYSTEMS, MAB0601), anti-GFP (Proteintech, 66002-1-Ig), anti-Lamin B1 (Cell Signaling, 12586S), and anti-alpha Tubulin (Proteintech, 11224-1-AP), each at 1:1000. After washing three times in TBST, 5 min each, the membrane was reacted with the following secondary antibodies: ECL Anti-mouse IgG, Horseradish Peroxidase linked whole antibody (GE Healthcare NA931V) and Cytiva's Amersham ECL Rabbit IgG, HRP-linked whole Ab (GE Healthcare NA934). The signal was visualized and scanned with ImageQuant LAS 4000 (GE Healthcare). Quantitative comparison of the band intensity was analyzed by ImageJ.

Immunofluorescent analysis

HeLa cells (3×10^5) were plated on coverslips, incubated overnight, and transfected with DNA constructs using FuGENE HD. Twenty-four hours after transfection, the cells were treated with IFNγ (100 U/ml) (Peprotech, AF-300-02-100UG), LMB (LC Laboratories, L-6100) or ivermectin (FUJIFILM Wako Pure Chemical Corporation, 70288-86-7) alone or their collaboration. The cells were then fixed with 4% paraformaldehyde for 20 min at 4 °C, permeabilized with 0.05% Triton X-100 in PBS for 5 min at room temperature, blocked with 5 mg/ml bovine serum albumin in PBST (0.04% Tween20 in PBS) for 30 min, and incubated with primary antibodies (anti-FLAG (Sigma, SL05105), anti-HA (B&D SYSTEMS, MAB0601), anti-GFP (Proteintech, 66002-1-Ig)) overnight at 4 °C. Subsequently, the cells were incubated with secondary antibodies (Goat anti-Mouse IgG (H&L) - Alexa Fluor 488 (Invitrogen, A-11001), Goat anti-Rabbit IgG (H&L) – Alexa Fluor 594 (Invitrogen, A-11012)) for 1 h at 22 °C. The nuclei were stained with 1 μg/ml of Hoechst 33342 and analyzed using a confocal laser microscope (Olympus). Quantitative comparison of the nuclear NLRC5 signal intensity (% of nuclear signal intensity/total cell signal intensity) was analyzed by ImageJ, the whole cell or the cell nucleus was selected using the "freehand" tool, and the integrated density was measured for each region of interest.

RNA isolation and RT-qPCR

For the evaluation of mRNA expression, RNA was reverse transcribed into cDNA using ReverTra Ace qPCR RT Master Mix reagent (Toyobo) according to the manufacturer's protocol, and RT-qPCR was performed using THUNDERBIRDTM SYBRTM qPCR Mix reagent (Toyobo) with the specific primer sets targeting human NLRC5 (hNLRC5-Fw: CTGGCCAGTCTCACCGCACAA, hNLRC5-Rv: CCAGGGGACAGCCATCAAAATC), HLA-A (hHLA-A-Fw: AAAAGGAGGGAGTTACACTCAGG, hHLA-A-Rv: GCTGTGAGGGACACATCAGAG), HLA-B (hHLA-B-Fw: CTACCCTGCGGAGATCA, hHLA-B-Rv: ACAGCCAGGCCAGCAACA), TAP1 (hTAP1-Fw: AGGGCTGGCTGGCTGCTTTGA, hTAP1-Rv: ACGTGGCCCATGGTGTTGTTAT), B2M (hB2M-Fw: TGCTGTCTCCATGTTTGATGTATCT, hB2M-Rv: TCTCTGCTCCCCACCTCTAAGT), and GAPDH (hGAPDH-Fw: GAAGGTGAAGGTCGGAGT, hGAPDH-Rv: GAAGATGGTGATGGGATTTC). The relative expression of each mRNA normalized by GAPDH was determined using the ΔΔCt method. Fold-change compared to control cells in the expression of the indicated genes represents the mean (±SD) of triplicate reactions.

Luciferase reporter assays

For the luciferase assays, 1×10^4 HEK293T cells were plated in one well in a 48-well plate. The cells were transfected with a mixture of 150 ng of pGL3-HLA-B and 10 ng of pRL-TK using the FuGENE HD Transfection Reagent following the manufacturer's protocol. After 48 h of transfection, the cells were treated with 100 nM of LMB for 8 h and then harvested for luciferase activity measurements.

Statistics

Statistical analyses were performed by a Two-tailed unpaired *t* test. The result significance was indicated as $^{*}p < 0.05$; $^{**}p < 0.01$; $^{***}p < 0.001$; $^{****}p < 0.0001$; ns, not significant using data from three independent experiments. The error bars represent mean values ± SD. Analyses were carried out with GraphPad Prism (GraphPad Software).

Data availability

Data are contained within the article and its Supporting information.

Supporting information—This article contains supporting information.

Acknowledgments—The authors thank C. Matsukawa and K. Ogawa for secretarial assistance and Dr Ji-Seung Yoo for invaluable guidance and support for this project. We thank all members of the Department of Immunology of the Graduate School of Medicine at Hokkaido University for their support during this study. We thank Dr Peter Van den Elsen and Dr Shigetsugu Hatakeyama for providing reagents. This work was supported by Japan Society for the Promotion of Science (JSPS) KAKEN under grant numbers 19K21250, 20K21511, 22H02883, 22KK0112, 19K1668109, and 22K19415, the Japan Agency for Medical Research and Development (AMED) under Grants JP223fa627005 and 23ym0126801j0002, the Japan Science and Technology (JST)

START University Ecosystem Promotion Type under the grant number JPMJST2284, Takeda Science Foundation, Bristol-Myers Squibb, SENSHIN Medical Research Foundation, Hitachi Global Foundation, Kobayashi Foundation, and The Toyo Suisan Foundation.

Author contributions—B. Z. conceptualization; B. Z. methodology; B. Z., R. O., and N. A. investigation; B. Z. visualization; B. Z. writing–original draft; R. O., T. T., and K. S. K. writing–review and editing; K. S. K. supervision.

Funding and additional information—B. Z. is the recipient of a fellowship from China Scholarship Council.

Conflict of interest—The authors declare that they have no conflicts of interest with the contents of this article.

Abbreviations—The abbreviations used are: B2M, beta-2-microglobulin; CARD, caspase recruitment domain; CITA, MHC class I transactivator; CIITA, MHC class II transactivator; CRM, chromosome region maintenance; GCN5, general control non-repressed 5 protein; HAT, histone acetyltransferase; KPNA, karyopherin alpha; LMB, leptomycin B; LRR, leucine-rich repeat; MHC, major histocompatibility complex; NBD, nucleotide-binding domain; NES, nuclear export signal sequence; NLR, Nod-like receptor; NLRC5, NLR family, CARD domain-containing 5; NLS, nuclear localization signal; NPC, nuclear pore complex; PCAF, P300/CBP-associated factor; RT-qPCR, quantitative reverse-transcription PCR; TAP1, transporter associated with antigen processing 1.

References

1. Pamer, E., and Cresswell, P. (1998) Mechanisms of MHC class I–restricted antigen processing. *Annu. Rev. Immunol.* **16**, 323–358
2. Shastri, N., Cardinaud, S., Schwab, S. R., Serwold, T., and Kunisawa, J. (2005) All the peptides that fit: the beginning, the middle, and the end of the MHC class I antigen-processing pathway. *Immunol. Rev.* **207**, 31–41
3. van den Elsen, P. J., Gobin, S. J., van Eggermond, M. C., and Peijnenburg, A. (1998) Regulation of MHC class I and II gene transcription: differences and similarities. *Immunogenetics* **48**, 208–221
4. van den Elsen, P. J., Peijnenburg, A., van Eggermond, M. C., and Gobin, S. J. (1998) Shared regulatory elements in the promoters of MHC class I and class II genes. *Immunol. Today* **19**, 308–312
5. Dhatchinamoorthy, K., Colbert, J. D., and Rock, K. L. (2021) Cancer immune evasion through loss of MHC class I antigen presentation. *Front. Immunol.* **12**, 636568
6. Hewitt, E. W. (2003) The MHC class I antigen presentation pathway: strategies for viral immune evasion. *Immunology* **110**, 163–169
7. Meissner, T. B., Li, A., and Kobayashi, K. S. (2012) NLRC5: a newly discovered MHC class I transactivator (CITA). *Microbes Infect.* **14**, 477–484
8. Kobayashi, K. S., and van den Elsen, P. J. (2012) NLRC5: a key regulator of MHC class I-dependent immune responses. *Nat. Rev. Immunol.* **12**, 813–820
9. Ting, J. P., Lovering, R. C., Alnemri, E. S., Bertin, J., Boss, J. M., Davis, B. K., *et al.* (2008) The NLR gene family: a standard nomenclature. *Immunity* **28**, 285–287
10. Wilmanski, J. M., Petnicki-Ocwieja, T., and Kobayashi, K. S. (2008) NLR proteins: integral members of innate immunity and mediators of inflammatory diseases. *J. Leukoc. Biol.* **83**, 13–30
11. Meissner, T. B., Li, A., Biswas, A., Lee, K. H., Liu, Y. J., Bayir, E., *et al.* (2010) NLR family member NLRC5 is a transcriptional regulator of MHC class I genes. *Proc. Natl. Acad. Sci. U. S. A.* **107**, 13794–13799
12. Meissner, T. B., Li, A., Liu, Y. J., Gagnon, E., and Kobayashi, K. S. (2012) The nucleotide-binding domain of NLRC5 is critical for nuclear import and transactivation activity. *Biochem. Biophys. Res. Commun.* **418**, 786–791
13. Braun, T., Schofield, P. R., and Sprengel, R. (1991) Amino-terminal leucine-rich repeats in gonadotropin receptors determine hormone selectivity. *EMBO J.* **10**, 1885–1890
14. Kobe, B., and Deisenhofer, J. (1993) Crystal structure of porcine ribonuclease inhibitor, a protein with leucine-rich repeats. *Nature* **366**, 751–756
15. Motyan, J. A., Bagossi, P., Benko, S., and Tozser, J. (2013) A molecular model of the full-length human NOD-like receptor family CARD domain containing 5 (NLRC5) protein. *BMC Bioinformatics* **14**, 275
16. Boss, J. M., and Jensen, P. E. (2003) Transcriptional regulation of the MHC class II antigen presentation pathway. *Curr. Opin. Immunol.* **15**, 105–111
17. Masternak, K., Muhlethaler-Mottet, A., Villard, J., Zufferey, M., Steimle, V., and Reith, W. (2000) CIITA is a transcriptional coactivator that is recruited to MHC class II promoters by multiple synergistic interactions with an enhanceosome complex. *Genes Dev.* **14**, 1156–1166
18. Steimle, V., Siegrist, C. A., Mottet, A., Lisowska-Grospierre, B., and Mach, B. (1994) Regulation of MHC class II expression by interferon-gamma mediated by the transactivator gene CIITA. *Science* **265**, 106–109
19. LeibundGut-Landmann, S., Waldburger, J. M., Krawczyk, M., Otten, L. A., Suter, T., Fontana, A., *et al.* (2004) Mini-review: Specificity and expression of CIITA, the master regulator of MHC class II genes. *Eur. J. Immunol.* **34**, 1513–1525
20. Cressman, D. E., O'Connor, W. J., Greer, S. F., Zhu, X. S., and Ting, J. P. (2001) Mechanisms of nuclear import and export that control the subcellular localization of class II transactivator. *J. Immunol.* **167**, 3626–3634
21. Lange, A., Mills, R. E., Lange, C. J., Stewart, M., Devine, S. E., and Corbett, A. H. (2007) Classical nuclear localization signals: definition, function, and interaction with importin alpha. *J. Biol. Chem.* **282**, 5101–5105
22. Chi, N. C., Adam, E. J., and Adam, S. A. (1995) Sequence and characterization of cytoplasmic nuclear protein import factor p97. *J. Cell Biol.* **130**, 265–274
23. Gorlich, D., and Mattaj, I. W. (1996) Nucleocytoplasmic transport. *Science* **271**, 1513–1518
24. Miyamoto, Y., Hieda, M., Harreman, M. T., Fukumoto, M., Saiwaki, T., Hodel, A. E., *et al.* (2002) Importin alpha can migrate into the nucleus in an importin beta- and Ran-independent manner. *EMBO J.* **21**, 5833–5842
25. Fornerod, M., Ohno, M., Yoshida, M., and Mattaj, I. W. (1997) CRM1 is an export receptor for leucine-rich nuclear export signals. *Cell* **90**, 1051–1060
26. Fukuda, M., Asano, S., Nakamura, T., Adachi, M., Yoshida, M., Yanagida, M., *et al.* (1997) CRM1 is responsible for intracellular transport mediated by the nuclear export signal. *Nature* **390**, 308–311
27. Wolff, B., Sanglier, J. J., and Wang, Y. (1997) Leptomycin B is an inhibitor of nuclear export: inhibition of nucleo-cytoplasmic translocation of the human immunodeficiency virus type 1 (HIV-1) Rev protein and Rev-dependent mRNA. *Chem. Biol.* **4**, 139–147
28. Fruh, K., and Yang, Y. (1999) Antigen presentation by MHC class I and its regulation by interferon gamma. *Curr. Opin. Immunol.* **11**, 76–81
29. Baldeon, M. E., Neece, D. J., Nandi, D., Monaco, J. J., and Gaskins, H. R. (1997) Interferon-gamma independently activates the MHC class I antigen processing pathway and diminishes glucose responsiveness in pancreatic beta-cell lines. *Diabetes* **46**, 770–778
30. Fujimaki, H., Hikawa, N., Nagoya, M., Nagata, T., and Minami, M. (1996) IFN-gamma induces expression of MHC class I molecules in adult mouse dorsal root ganglion neurones. *Neuroreport* **7**, 2951–2955
31. Zhou, F. (2009) Molecular mechanisms of IFN-gamma to up-regulate MHC class I antigen processing and presentation. *Int. Rev. Immunol.* **28**, 239–260
32. Yoo, J. S., Sasaki, M., Cho, S. X., Kasuga, Y., Zhu, B., Ouda, R., *et al.* (2021) SARS-CoV-2 inhibits induction of the MHC class I pathway by targeting the STAT1-IRF1-NLRC5 axis. *Nat. Commun.* **12**, 6602
33. Hake, S. B., Masternak, K., Kammerbauer, C., Janzen, C., Reith, W., and Steimle, V. (2000) CIITA leucine-rich repeats control nuclear

localization, *in vivo* recruitment to the major histocompatibility complex (MHC) class II enhanceosome, and MHC class II gene transactivation. *Mol. Cell. Biol.* **20**, 7716–7725
34. Meissner, T. B., Liu, Y. J., Lee, K. H., Li, A., Biswas, A., van Eggermond, M. C., *et al.* (2012) NLRC5 cooperates with the RFX transcription factor complex to induce MHC class I gene expression. *J. Immunol.* **188**, 4951–4958
35. Spilianakis, C., Papamatheakis, J., and Kretsovali, A. (2000) Acetylation by PCAF enhances CIITA nuclear accumulation and transactivation of major histocompatibility complex class II genes. *Mol. Cell. Biol.* **20**, 8489–8498
36. Maharana, J., Panda, D., and De, S. (2018) Deciphering the ATP-binding mechanism(s) in NLRP-NACHT 3D models using structural bioinformatics approaches. *PLoS One* **13**, e0209420
37. Mo, J., and Duncan, J. A. (2013) Assessing ATP binding and hydrolysis by NLR proteins. *Methods Mol. Biol.* **1040**, 153–168
38. Lew, Q. J., Chu, K. L., Chia, Y. L., Soo, B., Ho, J. P., Ng, C. H., *et al.* (2015) GCN5 inhibits XBP-1S-mediated transcription by antagonizing PCAF action. *Oncotarget* **6**, 271–287
39. Nickerson, K., Sisk, T. J., Inohara, N., Yee, C. S., Kennell, J., Cho, M. C., *et al.* (2001) Dendritic cell-specific MHC class II transactivator contains a caspase recruitment domain that confers potent transactivation activity. *J. Biol. Chem.* **276**, 19089–19093
40. Benko, S., Magalhaes, J. G., Philpott, D. J., and Girardin, S. E. (2010) NLRC5 limits the activation of inflammatory pathways. *J. Immunol.* **185**, 1681–1691
41. Vijayan, S., Sidiq, T., Yousuf, S., van den Elsen, P. J., and Kobayashi, K. S. (2019) Class I transactivator, NLRC5: a central player in the MHC class I pathway and cancer immune surveillance. *Immunogenetics* **71**, 273–282
42. Xu, W., Edmondson, D. G., and Roth, S. Y. (1998) Mammalian GCN5 and P/CAF acetyltransferases have homologous amino-terminal domains important for recognition of nucleosomal substrates. *Mol. Cell. Biol.* **18**, 5659–5669
43. Gobin, S. J., van Zutphen, M., Westerheide, S. D., Boss, J. M., and van den Elsen, P. J. (2001) The MHC-specific enhanceosome and its role in MHC class I and beta(2)-microglobulin gene transactivation. *J. Immunol.* **167**, 5175–5184